EJNMMI Research

ORIGINAL RESEARCH

Open Access

Comparison between [^{68}Ga]Ga-FAPI-46 and [^{18}F]FDG PET/CT uptake in luminal-like vs. HER2-positive breast cancer

Alina Toni Küper[1*†], Sofia Carrilho Vaz[2,3†], Kim Magaly Pabst[1], Ieva Ciuciulkaite[1], Ilektra Antonia Mavroeidi[4], Rainer Hamacher[2], Anja Welt[4,5], Noah Hammersen[1], Pedro Fragoso Costa[1], Loic Djaileb[6], Robert Seifert[7], Lale Umutlu[8], Martin Schuler[4,5], Ken Herrmann[1], Wolfgang Peter Fendler[1,4,5], Sherko Kümmel[9] and David Kersting[1]

Abstract

Background Fibroblast activation protein (FAP)–targeted tracers have emerged as promising agents for breast cancer imaging, with recent studies demonstrating PET performance comparable to or surpassing, that of [^{18}F]FDG. Nevertheless, data comparing [^{68}Ga]Ga-FAPI-46 and [^{18}F]FDG uptake in hormone receptor and/or HER2–positive breast cancer (luminal-like vs HER2-positive) remain scarce. Aim of this study was to investigate the diagnostic performance of [^{68}Ga]Ga-FAPI-46 versus [^{18}F]FDG PET/CT in patients with hormone-receptor and/or HER2-positive breast cancer, and to evaluate the uptake of both tracers stratified by molecular subtypes (luminal-like vs HER2-positive). A sub-analysis of a prospective observational trial (NCT04571086) was conducted. Patients with histologically confirmed, hormone receptor- and/or HER2-positive breast cancer who underwent whole-body [^{68}Ga]Ga-FAPI-46 and [^{18}F]FDG PET/CT in the same week for initial staging or follow-up were included. [^{68}Ga]Ga-FAPI-46 or [^{18}F]FDG PET-positive lesions were defined as visually increased lesion uptake compared to adjacent organ background. Semi-automatic segmentation was performed to determine SUVmax, SUVpeak, TLRpeak, total number of lesions, total tumour volume, and total tumour SUV mean. Data were compared between molecular subtypes (luminal-like vs HER2-positive).

Results Thirteen patients were included. Overall, the detection performance was comparable between [^{68}Ga]Ga-FAPI-46 and [^{18}F]FDG PET. The semi-quantitative analysis showed comparable mean uptake values in breast cancer lesions on [^{68}Ga]Ga-FAPI-46 and [^{18}F]FDG PET/CT (SUV_{max}: 13.4 vs. 12.9; TLR_{peak}: 5.6 vs. 4.5) and revealed no significant differences in the median lesion count (4.5 vs. 5), mean total tumour volume (71.5 vs. 73.2 mL), or mean total tumour SUV_{mean} (5.4 vs. 5.4). No substantial differences between molecular subtypes (luminal-like vs. HER2-positive) were observed.

†Alina Toni Küper and Sofia Carrilho Vaz contributed equally to this work.

*Correspondence:
Alina Toni Küper
Alina.Kueper@uk-essen.de

Full list of author information is available at the end of the article

Conclusion In this small exploratory cohort, comparable uptake patterns in [^{68}Ga]Ga-FAPI-46- and [^{18}F]FDG-positive breast cancer lesions were observed across subtypes, underscoring the potential of [^{68}Ga]Ga-FAPI-46 as a versatile imaging tool. Future studies in larger cohorts are warranted to explore the potential of FAP-targeted theranostics in different breast cancer subtypes.

Trial registration 68-Ga-FAPI-PET for Tumor Detection: A Prospective Observational Trial, NCT04571086, 09-15-2020, https://clinicaltrials.gov/study/NCT04571086.

Keywords Breast cancer, PET, FDG, FAPI, Pan-tumour imaging, Hormone receptors, Luminal-like, HER2, Theranostics

Introduction

Breast cancer is the most common cancer in women worldwide. In 2022 it was the second most frequently diagnosed cancer and the leading cause of cancer-related death in women [1]. By 2040, breast cancer is predicted to increase to over 3 million new cases and 1 million deaths per year, being a major health concern [2].

Breast cancer is a heterogenous disease, characterized by diverse biological features and clinical presentations. The main molecular subtypes are Luminal A-like in 50/60% (hormone receptor (HR)-positive, HER2-negative and low-grade/low proliferation), Luminal B-like in 15/20% (HR-positive, HER2-negative and high-grade/high proliferation) and HER2-positive in 10/15% of cases (HR-positive or negative and HER2-positive) [3, 4]. Breast cancer is usually staged according to the Union for International Cancer Control (UICC) in primary tumour, nodal status and distant metastases (TNM) classification [5].

Imaging is essential for staging. Mammography, sonography, and MRI are often used for locoregional assessment. Despite significant developments and promising results from molecular imaging modalities, they are mainly used in ambiguous cases or systemic staging in advanced disease [6]. Although [^{18}F]fluorodeoxyglucose (FDG) remains the most widely used positron emission tomography (PET) tracer for systemic staging in breast cancer, its performance is constrained by several well-recognised limitations. These include reduced sensitivity for small lesions, micrometastatic disease, hormone receptor-positive tumours, and lobular subtype. This limitation is well documented for luminal A and, to a lesser extent, luminal B tumours, which show lower [^{18}F]FDG-avidity than HER2-positive or triple-negative cancers. FDG uptake is also prone to false positive results, particularly after biopsy or in benign breast conditions such as infection, fibroadenoma, or ductal adenoma [7, 8].

Recent literature has demonstrated promising results with more specific tracers such as [^{18}F]fluoroestradiol (FES) for estrogen receptor-positive tumours and [^{89}Zr] trastuzumab for HER2-positive disease [9, 10]. Nevertheless, these tracers are not widely available and seem particularly useful in selecting patients for targeted therapy [11, 12].

In contrast, fibroblast activation protein inhibitor (FAPI) based tracers (e.g., [^{68}Ga]Ga-FAPI-46) are emerging compounds that may provide advantageous imaging properties across all breast cancer subtypes, as they visualise cancer-associated fibroblasts (CAFs) and thereby reflect stromal remodelling and desmoplasia [13, 14]. Fibroblast activation protein (FAP) is highly expressed on the membrane of CAFs, which is the most abundant component of the tumour microenvironment, and can contribute to tumour angiogenesis, migration, and invasion of tumour cells [15, 16]. Several studies have demonstrated the benefit of using FAP tracers for the detection of breast cancer lesions, reporting potentially higher sensitivity, maximum standardized uptake values (SUV_{max}), and tumour-to-background ratios compared to [^{18}F]FDG [14, 17–20]. Moreover, FAP tracers were superior to [^{18}F] FDG in in identifying lymph node, hepatic, bone, and brain metastases [14, 21]. There are increasing expectations about the use of FAP tracers as a pan-tumour marker with theranostic potential, including in breast cancer [13, 22–25].

Despite a growing number of studies comparing the diagnostic performance of [^{18}F]FDG and [^{68}Ga]Ga-FAP tracers in breast cancer, most investigations assess breast cancer as a single entity-without stratifying by hormone receptors or HER2 expression. Exceptions are limited to a few studies specifically addressing the lobular subtype [26, 27] and a small number focusing on triple-negative breast cancer [28, 29]. Consequently, data comparing [^{68}Ga]Ga-FAPI-46 and [^{18}F]FDG uptake in luminal-like and HER2-positive breast cancer remain scarce.

The aim of this study was to investigate the diagnostic performance of [^{68}Ga]Ga-FAPI-46 versus [^{18}F]FDG PET/CT in patients with hormone receptor- and/or HER2-positive positive breast cancer. As a secondary objective, we evaluated [^{68}Ga]Ga-FAPI-46 and [^{18}F]FDG PET/CT uptake stratified by molecular subtypes (luminal-like vs. HER2-positive).

Methods

Patients and ethics

A sub-analysis of the prospective University Hospital Essen [^{68}Ga]Ga-FAPI-46 PET observational trial (NCT04571086) was conducted. Patients with

histologically confirmed, hormone receptor- and/or HER2-positive breast cancer who underwent clinically indicated whole-body [^{18}F]FDG and [^{68}Ga]Ga-FAPI-46 PET/CT in the same week for initial diagnostic workup or follow-up staging between October 2021 and April 2025 were consecutively included. The clinically requested FAPI examination routinely entailed complementary [^{18}F]FDG PET/CT imaging according to institutional standards. Patient referrals were made by the treating gynaecologic oncologists. If patients were scanned with [^{68}Ga]Ga-FAPI-46 PET/CT more than once, only the first paired examination was included. Patients with triple negative breast cancer and those without any [^{68}Ga]Ga-FAPI-46 or [^{18}F]FDG positive lesions were excluded from further analysis. Patients were categorized according to hormone receptor and HER2 expression into luminal A-like, luminal-B like and HER2-positive (including the HER2-enriched subtype). For subsequent analyses, luminal A-like and luminal B-like tumours were combined into a single hormone receptor-positive group due to the limited number of patients in each individual subtype. Written informed consent for study participation and to undergo clinical PET examinations were obtained from all patients. All investigations were conducted in accordance with the Declaration of Helsinki and national regulations. The local institutional ethics committee (University of Duisburg–Essen, medical faculty) approved the study (ethics protocol permits 19–8991-BO and 20–9485-BO).

[^{68}Ga]Ga-FAPI-46 and [^{18}F]FDG PET/CT imaging

PET/CT images were acquired on a Biograph Vision 600 or a Biograph mCT PET/CT system (both Siemens Healthineers, Erlangen, Germany). The mean [^{68}Ga]Ga-FAPI-46 administered activity was 104 MBq (62–144) and the mean uptake time was 20 min (10–99). The mean [^{18}F]FDG administered activity was 231 MBq (82–377) and the mean uptake time was 101 min (53–305). According to institutional protocols, patients underwent a contrast-enhanced whole-body CT scan prior to PET, provided such an exam had not already been performed within the previous four weeks. If a recent CT was available, a low-dose, non-contrast CT was instead acquired and used for attenuation correction and anatomical localization of PET uptake. PET data were acquired and PET images were reconstructed according to our standard institutional protocols [30].

PET image interpretation

All PET images were analyzed separately by three nuclear medicine physicians using Syngo.via software (version VB80D; Siemens Healthineers). In cases of divergent findings, the images were reexamined to establish a consensus. Nuclear medicine physicians confirmed imaging quality. Patient-based and region-based analysis for [^{68}Ga]Ga-FAPI-46 or [^{18}F]FDG PET-positive lesions were reported for each patient separately. Six different anatomic categories derived from the UICC TNM classification for breast cancer were defined [5]: primary tumour, regional lymph node metastases, distant lymph node metastases, liver metastases, bone metastases and other distant metastases.

Lesions were classified as metastatic if they showed abnormal radiotracer uptake in a typical metastatic location or when uptake was low but an anatomically matching abnormality was detectable on CT. In case of unclear interpretation of lesion uptake, clinical information, blood test and other imaging modalities were considered, as biopsy was not performed. The final interpretation of the PET/CT examination was subsequently reviewed in an interdisciplinary tumour board to ensure consensus assessment. [^{68}Ga]Ga-FAPI-46-/[^{18}F]FDG-positivity was defined as visually markedly increased lesion uptake compared to adjacent organ background. Brain metastases were described but not included into quantitative analysis due to the high physiologic cerebral [^{18}F]FDG uptake, which limits lesion identification. Additionally, the skull is not included in the standard scan field of view of contrast-enhanced PET protocols for oncologic PET/CT imaging at our institution.

Lesion analysis and quantification

Semi-automatic segmentation of all [^{68}Ga]Ga-FAPI-46- and/or [^{18}F]FDG PET-positive lesions per patient was performed, using a PERCIST-like approach considering a liver-specific threshold defined as lesion peak standard uptake value (SUV_{peak}) that was required to be at least (1.5 x SUV_{mean} liver + 2 x standard deviation (SD) of SUV liver) [31]. Liver SUV_{mean} values were determined in a spherical volume-of-interest of 14 mL volume (3-cm diameter) in the right liver lobe as suggested in PERCIST 1.0. Lesion boundaries were determined using a 41% isocontour approach [32]. Small lesions with a volume below 0.5 ml were excluded. Additional foci with lower SUV values were manually included when required, while physiologic uptake was manually excluded. Lesion SUV_{max}, SUV_{peak}, tumour-to-liver ratio $_{peak}$ (TLR_{peak}), total number of lesions, total tumour volume (sum of the volumes of all [^{68}Ga]Ga-FAPI-46 or [^{18}F]FDG PET-positive lesions), and total tumour SUV_{mean} (SUV_{mean} in the entire total tumour volume) were determined.

Statistics

All statistical analyses were conducted using IBM Statistical Package for the Social Sciences (SPSS) Statistics software (version 29.0.0, IBM Corp., Armonk, N.Y., USA). Mean values were presented as mean ± standard deviation (SD). The Shapiro-Wilk test was applied to verify

normal distribution. To compare [^{68}Ga]Ga-FAPI-46 and [^{18}F]FDG uptake (analyzing the total number of detected lesions, total tumour volume, and mean global SUV_{mean}), Kruskal-Wallis Test was employed. To compare [^{68}Ga]Ga-FAPI-46 and [^{18}F]FDG uptake in each location of the luminal-like and HER2-positive groups (analyzing the SUV_{max} and TLR_{peak}), the independent samples Mann-Whitney U Test was used. P-values (P) < 0.05 were considered statistically significant. The SUV_{max} and TLR_{peak} percentage differences between [^{68}Ga]Ga-FAPI-46 and [^{18}F]FDG uptake were calculated for each involved region and sub-category (luminal-like or HER2-positive).

Results

Patient and tumour characteristics

Thirteen women were included, the mean age was 57 years (ranging from 34 to 74 years). All patient except one underwent both [^{68}Ga]Ga-FAPI-46 and [^{18}F]FDG PET scans on the same day. In one case, [^{68}Ga]Ga-FAPI-46 PET was conducted seven days before [^{18}F]FDG PET for logistical reasons, with no invasive procedures or treatments undertaken between the examinations. In two patients, both PET/CT examinations were performed at baseline staging; in all other patients, scans were acquired during follow-up due to rising tumour markers or clinical-/imaging based suspicion of disease progression or resistance to therapy. The majority of patients had no special type breast cancer (8/13) and moderately (7/13) or poorly differentiated (6/13) cancer. One half had luminal-like breast cancer and the other half had HER2-positive breast cancer (detailed information about receptor status, HER2 and Ki-67 per patient is provided in Table 1 from the supplementary material). At baseline staging, four patients were classified UICC 4 and three patients UICC 1. In the majority of patients (10/13), tumour metastases were already known before the PET scan. Most patients were submitted to surgery and received systemic therapy before performing PET/CT (Table 1).

Table 1 Patient and breast cancer characteristics

Mean age (min-max)	**57 (34–74)**
Subtype	
No special type	8
Lobular	4
NA	1
Hormone Receptors & HER2 expression	
Luminal A-like	2
Luminal B-like	4
HER2-positive	6
Luminal A/HER2	1 (*)
Differentiation grade	
G1	0
G2	7
G3	6
UICC staging at baseline	
1	3
2a	2
2b	2
3c	2
4	4
Known metastasis when performing PET	
No metastatic disease	3
Metastatic disease	10
Treatment	
Naive	3
Breast surgery	8
Targeted therapy	9
Chemotherapy	6
Adjuvant radiation therapy	5
Additional radiation therapy (**)	4

(*) bilateral breast cancer (luminal A-like on the left side and HER2-positive on the right side).

(**) due to relapse in the axilla and chest wall

[^{68}Ga]Ga-FAPI-46 and [^{18}F]FDG PET detection performance

Overall, the detection performance was comparable between [^{68}Ga]Ga-FAPI-46 and [^{18}F]FDG PET with [^{68}Ga]Ga-FAPI-46 PET showing slight advantages for detection of distant metastases. In detail, uptake in the breast region was observed on both [^{68}Ga]Ga-FAPI-46 and [^{18}F]FDG PET/CT in five patients. Both modalities detected local lymph node involvement in three cases. In addition, [^{68}Ga]Ga-FAPI-46 PET/CT revealed two further lesions, while [^{18}F]FDG PET/CT identified three additional lesions. Distant lymph node metastases were visualized in three patients on both scans, and in two additional patients with [^{68}Ga]Ga-FAPI-46 PET/CT only. Bone metastases showed concordant uptake in five patients. Additional metastatic sites with uptake on both PET/CT scans included the lung, liver, adrenal glands, and soft tissue in six patients. Among four patients with detected peritoneal metastases, one showed uptake exclusively on [^{68}Ga]Ga-FAPI-46 PET/CT despite the presence of a morphological correlate on CT. In two patients, leptomeningeal and brain metastases were visible on [^{68}Ga]Ga-FAPI-46 PET/CT. These findings could not be assessed on [^{18}F]FDG PET/CT, as the head was not included in the scan range. Figure 1 illustrates a representative case demonstrating comparable detection performance between [^{68}Ga]Ga-FAPI-46 and [^{18}F]FDG PET/CT.

In the semi-quantitative analysis, breast cancer lesions showed comparable mean SUV_{max} and TLR_{peak} values on [^{68}Ga]Ga-FAPI-46 and [^{18}F]FDG PET/CT (SUV_{max}: 13.4 ± 4.8 vs. 12.9 ± 14.2; TLR_{peak}: 5.6 ± 3.2 vs. 4.5 ± 5.4, respectively) (Table 2). Across the entire cohort, no significant differences were observed between the tracers regarding median lesion count (n: 4.5 vs. 5), mean total tumour volume (71.5 ± 87.2 mL vs. 73.2 ± 124.4 mL),

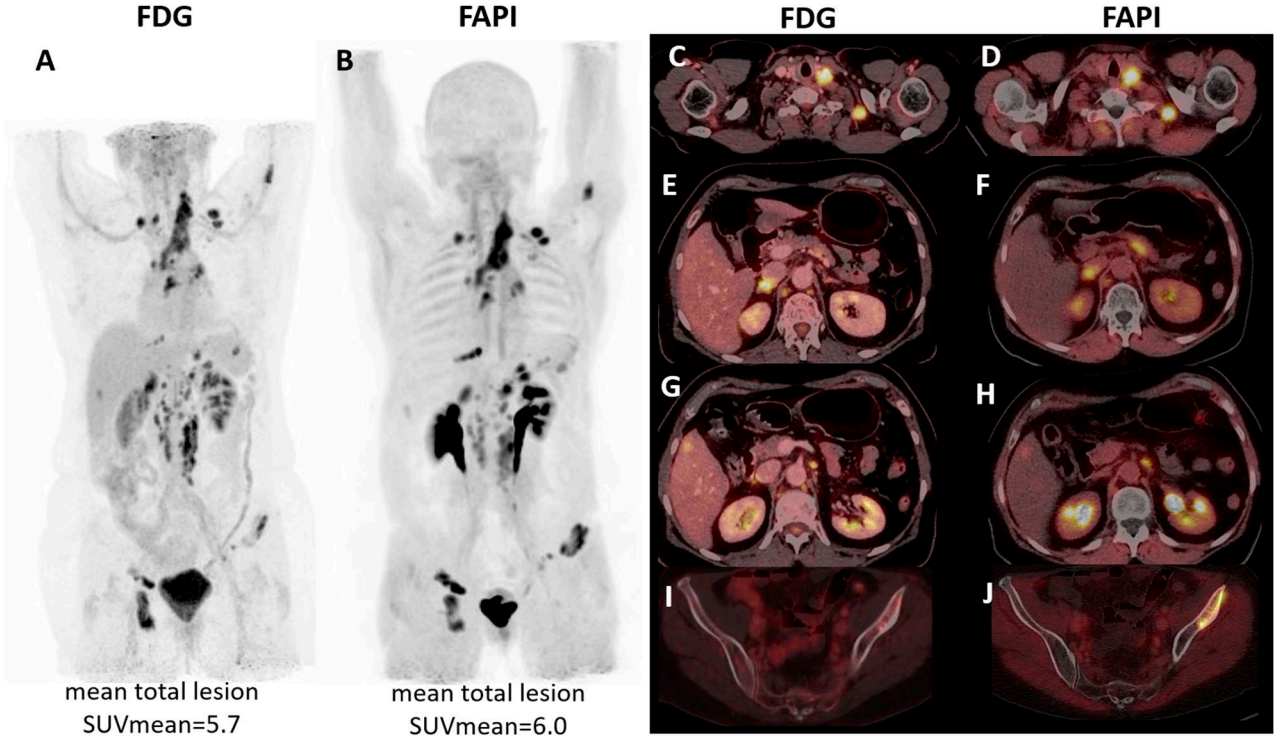

Fig. 1 Comparable detection performance of [^{18}F]FDG and [^{68}Ga]Ga-FAPI-46 PET/CT. 74 years old woman diagnosed with left-sided ductal luminal B-like breast cancer (UICC stage 2a). PET/CT showed pathologic uptake in local lymph nodes (SUV_{max} [^{18}F]FDG 11.0 vs. [^{68}Ga]Ga-FAPI-46 10.5 - **C**&**D**), liver (SUV_{max} [^{18}F]FDG 5.3 vs. [^{68}Ga]Ga-FAPI-46 3.1), adrenal gland (SUV_{max} [^{18}F]FDG 11.4 vs. [^{68}Ga]Ga-FAPI-46 8.6- **E**&**F**), distant lymph nodes (SUV_{max} [^{18}F]FDG 12.7 vs. [^{68}Ga]Ga-FAPI-46 14.2 - **G**&**H**), bone (SUV_{max} [^{18}F]FDG 13.9 vs. [^{68}Ga]Ga-FAPI-46 12.2 - **I**&**J**), peritoneal (SUV_{max} [^{18}F]FDG 8.9 vs. [^{68}Ga]Ga-FAPI-46 10.5), and leptomeningeal metastasis (SUV_{max} [^{68}Ga]Ga-FAPI-46 4.3, head not included in the [^{18}F]FDG PET/CT FOV). Overall lesions presented similar [^{18}F]FDG and [^{68}Ga]Ga-FAPI-46 uptake (mean total lesion SUV_{mean} on [^{18}F]FDG was 5.7 and [^{68}Ga]Ga-FAPI-46 was 6.0). **A**&**B** - PET maximum intensity projection; **C**-**J** - PET/CT fused transaxial plans

Table 2 [^{68}Ga]Ga-FAPI-46 and [^{18}F]FDG uptake per involved region

Involved regions		[^{68}Ga]Ga-FAPI-46			[^{18}F]FDG			Exclusive FAPI/FDG uptake
		Nº pts	SUV_{max}	TLR_{peak}	Nº pts	SUV_{max}	TLR_{peak}	
Breast		5	13.4 ± 4.8	5.6 ± 3.2	5	12.9 ± 14.2	4.5 ± 5.4	
Local lymph nodes		5	9.1 ± 6.9	**2.9 ± 1.8**	6	7.5 ± 6.5	**1.2 ± 1.3**	2 FAPI only 3 FDG only
M1	Distant lymph nodes	5	7.4 ± 4.6	3.3 ± 2.9	3	9.9 ± 5.1	2.6 ± 1.8	2 FAPI only
	Bone	5	**13.1 ± 6.4**	**6.3 ± 5.8**	5	**8.5 ± 5.5**	**2.0 ± 1.6**	
	Peritoneum	4	8.2 ± 5.3	**7.7 ± 5.4**	3	6.5 ± 2.5	**1.7 ± 0.7**	1 FAPI only
	Lung	1	5.5	2.2	1	6.9	1.2	
	Liver	1	3.1	1.6	1	5.3	3.8	
	Soft tissue	1	**7.6**	**3.2**	1	**42.3**	**14.0**	
	Adrenal gland	1	8.6	4.9	1	11.4	3.5	
								p-value
Nº of lesions		14.7 ± 20.0			18.9 ± 45.6			0.462
Total tumour volume		71.5 ± 87.2 mL			73.2 ± 124.4 mL			0.440
Total tumour SUV_{mean}		5.4 ± 2.7			5.4 ± 6.3			0.355

Data are presented as mean ± SD (median and min-max are provided in supplementary material: supplementary Table 2). Bold highlight percentage difference between [^{68}Ga]Ga-FAPI-46 and [^{18}F]FDG uptake ≥ 50% for each involved according to the expression of hormone receptors (supplementary material: supplementary Table 4).

or mean total tumour SUV_{mean} (5.4 ± 2.7 vs. 5.4 ± 6.3) (Table 2; Fig. 1).

Higher [^{68}Ga]Ga-FAPI-46 than [^{18}F]FDG uptake was observed in bone metastases (SUV_{max} 13.1 ± 6.4 vs. 8.5 ± 5.5 and TLR_{peak} 6.3 ± 5.8 vs. 2.0 ± 1.6). In a single patient with soft tissue metastasis, [^{18}F]FDG uptake was higher than [^{68}Ga]Ga-FAPI-46 (SUV_{max} 42.3 vs. 7.6 and TLR_{peak} 14.0 vs. 3.2) (Fig. 2).

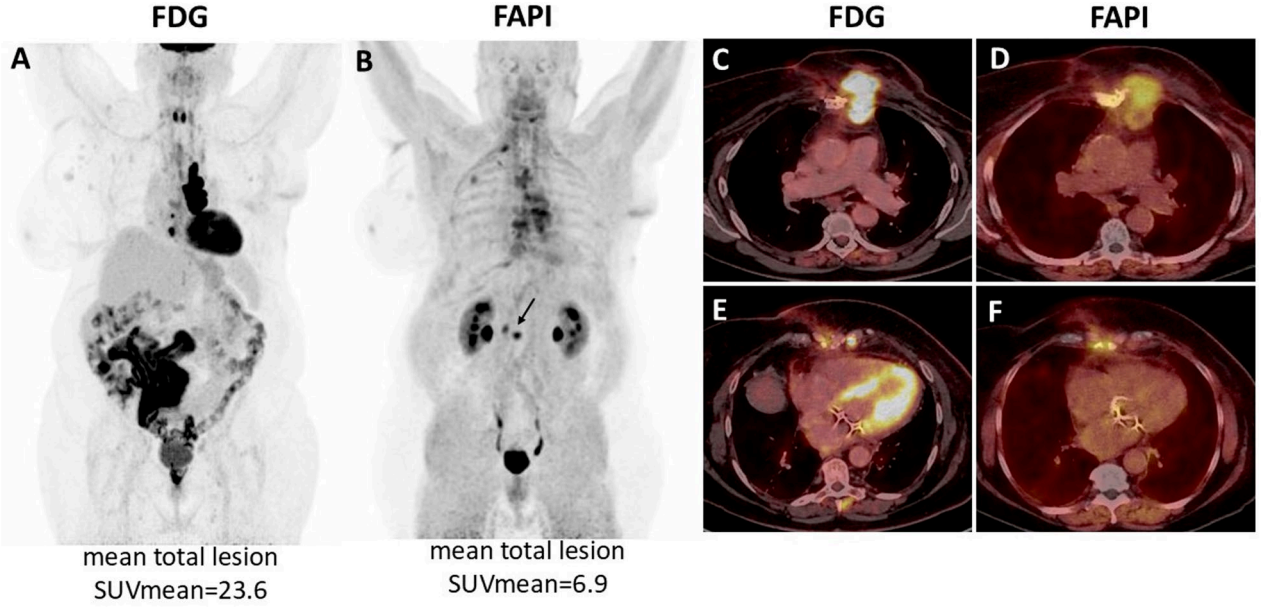

Fig. 2 Superior detection performance of [^{18}F]FDG PET/CT, compared to [^{68}Ga]Ga-FAPI-46 PET/CT. 65 years old woman diagnosed with left-sided ductal luminal B-like breast cancer (UICC stage 3c). PET/CT showed abnormal uptake in a soft tissue mass involving the left para-sternal region of the thoracic wall (SUV_{max} [^{18}F]FDG 42.3 vs. [^{68}Ga]Ga-FAPI-46 7.6 - **C**&**D**), internal mammary lymph nodes (SUV_{max} [^{18}F]FDG 18.9 vs. no [^{68}Ga]Ga-FAPI-46 uptake - **E**&**F**), and bone (SUV_{max} [^{18}F]FDG 4.1 vs. [^{68}Ga]Ga-FAPI-46 9.8 (arrow in **B**)). Overall lesions presented higher [^{18}F]FDG uptake than [^{68}Ga]Ga-FAPI-46 uptake (mean total lesion SUV_{mean} on [^{18}F]FDG 23.6 vs. [^{68}Ga]Ga-FAPI-46 6.9). **A**&**B** - PET maximum intensity projection; **C**-**F** - PET/CT fused transaxial plans

Generally, TLR was higher in [^{68}Ga]Ga-FAPI-46 than [^{18}F]FDG, particularly in local lymph nodes (6.1 ± 5.2 vs. 1.2 ± 1.3) and peritoneal metastases (7.7 vs. 1.7) (Fig. 3), as [^{68}Ga]Ga-FAPI-46 showed lower liver uptake than [^{18}F]FDG.

[^{68}Ga]Ga-FAPI-46 and [^{18}F]FDG PET detection performance across molecular subtypes

One patient presenting bilateral breast cancer (luminal-like on the left, HER2-positive on the right side; Table 1) was excluded from this sub-analysis, resulting in 12 evaluable patients. In general, no substantial differences between detection performances and uptake values of [^{68}Ga]Ga-FAPI-46 and [^{18}F]FDG across luminal-like and HER2-positive breast cancer was observed (Table 3).

Most metastatic lesions were observed in patients with luminal-like breast cancer. In the luminal-like sub-group, [^{18}F]FDG showed higher uptake than [^{68}Ga]Ga-FAPI-46 in breast lesions (SUV_{max}: 20.8 ± 23.3 vs. 9.6 ± 0.8; TLR_{peak}: 7.5 ± 9.2 vs. 4.1 ± 0.1) and in a single soft tissue metastasis (SUV_{max}: 42.3 vs. 7.6; TLR_{peak}: 14.0 vs. 3.2). Uptake in other distant metastases was comparable between [^{68}Ga]Ga-FAPI-46 and [^{18}F]FDG PET (Table 3).

Discussion

In this small exploratory cohort, the head-to-head comparison showed similar uptake patterns in [^{68}Ga]Ga-FAPI-46- and [^{18}F]FDG-positive breast cancer lesions of 13 patients with hormone receptor-positive and/or HER2-positive breast cancer. Overall, semi-quantitative comparison of lesion uptake on [^{68}Ga]Ga-FAPI-46 and [^{18}F]FDG PET/CT across the entire cohort, revealed no significant differences in the mean number of detected lesions, the mean total tumour volume, and the total tumour SUV_{mean} (Table 2).

Differences in detection rates of [^{18}F]FDG and FAP-targeted tracers across luminal A/B and HER2-positive breast cancer subtypes could reflect their distinct molecular targets and the specific features of the tumour microenvironment. [^{18}F]FDG primarily captures glucose metabolism through GLUT-mediated uptake and hexokinase activity, thereby imaging glycolytic activity (Warburg effect); while FAP tracers bind to CAFs traducing stromal remodelling and desmoplasia [33–35]. FAP is mainly secreted by adipose stromal CAFs, which are more prevalent in luminal A tumours, whereas HER2-positive, luminal B, and triple-negative cancers typically exhibit a more fibrotic stromal architecture [17, 36]. Some authors speculate that, in breast cancer, tumour-surrounding adipocytes may act as key precursors of CAFs, with breast cancer cells altering adjacent adipocytes, leading to reduced lipid content and up-regulation of fibroblast markers (including FAP) [36].

As FAP tracers mark a different biological process, they may complement [^{18}F]FDG, especially in low-FDG-avid tumours (such as luminal A, and to a lesser extent luminal B) [33, 37]. However, available data remain heterogeneous: some studies report high FAP uptake in

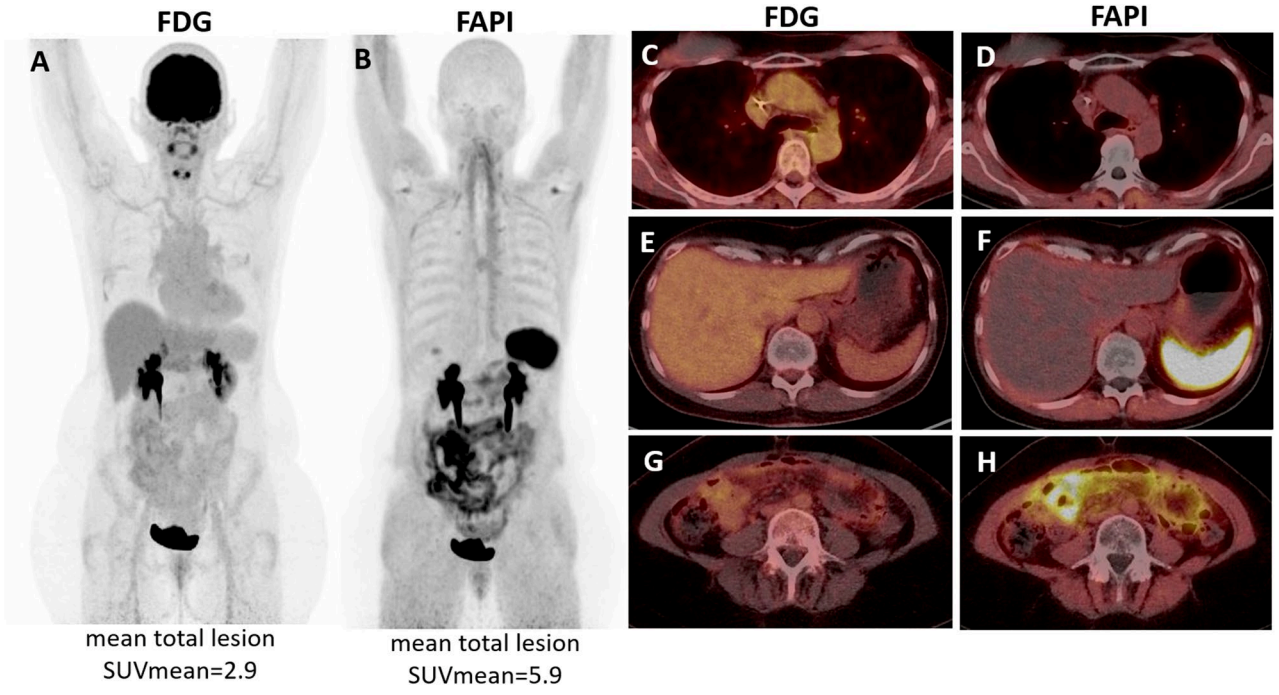

Fig. 3 Superior detection performance of [^{68}Ga]Ga-FAPI-46 PET/CT, compared to [^{18}F]FDG PET/CT. 54 years old woman diagnosed with right-sited lobular luminal A-like breast cancer (UICC stage 2a). PET/CT showed pathologic uptake in distant lymph nodes (at the mediastinum SUV_{max} [^{68}Ga]Ga-FAPI-46 2.4, no [^{18}F]FDG uptake - **C**&**D**) and peritoneal metastases (SUV_{max} [^{68}Ga]Ga-FAPI-46 14 vs. [^{18}F]FDG 4 - **G**&**H**). Overall, lesions presented higher [^{68}Ga]Ga-FAPI-46 uptake than [^{18}F]FDG (mean total lesion SUV_{mean} on [^{68}Ga]Ga-FAPI-46 5.9 vs. [^{18}F]FDG 2.9). Intense diffuse [^{68}Ga]Ga-FAPI-46 spleen uptake, probably therapy-related is observed (**F**). Seven months before PET, the patient had been submitted to abdominal surgery due to ileus and ascites, in which peritoneal carcinomatosis was diagnosed. **A**&**B** - PET maximum intensity projection; **C**-**H** - PET/CT fused transaxial plans

luminal A and HER2-positive subtypes [18], whereas other describe relatively low uptake in luminal A and B subtypes [38]. Although mapping different mechanisms, within our cohort, comparable uptake of [^{68}Ga]Ga-FAPI-46 and [^{18}F]FDG was observed across luminal-like and HER2-positive breast cancer cases. This is consistent with few previous reports showing no substantial differences in FAP uptake regardless of breast cancer histopathological characteristics, including immunohistochemistry, molecular features, and tumour grade [14, 18, 35, 39]. While we observed non-inferiority of [^{68}Ga]Ga-FAPI-46 compared to [^{18}F]FDG, a limited number of studies described superiority of using FAP-targeted tracers in breast cancer staging. However, these studies did not identify differences when stratifying by hormone receptor status or HER2 expression. Guo et al. [35] performed a prospective trial with 61 patients, comprising cases of newly diagnosed or suspected breast cancer before initiation of therapy, along with patients presenting with suspected recurrence or metastatic disease. They reported a higher lesion-based detection rate for FAP-targeted tracers compared with [^{18}F]FDG, resulting in changes in TNM staging in 22% (13/59) of patients and modifications in clinical management in 15% (9/59). They reported no significant differences in SUV_{max} values derived from either [^{18}F]FDG or FAP tracers across receptor-defined subgroups (HR-positive, HR-positive/HER2-positive, HER2-positive, and triple-negative). Median SUV_{max} values for [^{68}Ga]Ga-FAPI-46/[^{18}F]FAPI-42 compared with [^{18}F]FDG in primary breast tumours were consistently higher across all molecular subtypes – 9.6 vs. 2.3 in luminal A, 12.5 vs. 5.0 in luminal B, 12.9 vs. 7.0 in HER2-positive, and 12.4 vs. 3.3 in triple-negative disease. In our study, the median (range) SUV_{max} values for [^{68}Ga]Ga-FAPI-46 versus [^{18}F]FDG in luminal-like tumours were 9.7 (9.1–10.2) versus 20.8 (4.3–37.3), and in HER2-positive tumours 18.5 (10.3–18.7) versus 9.9 (1.4–11.7). Elboga et al. [18], retrospectively compared [^{68}Ga]Ga-FAPI-04 and [^{18}F]FDG uptake in 48 patients with breast cancer, irrespective of whether they had received chemotherapy within the previous month. They found that [^{68}Ga]Ga-FAPI-04 detected a greater number of lesions and showed higher uptake values than [^{18}F]FDG. They also reported no statistical significance related to the breast cancer pathological characteristics. In their study, the following [^{68}Ga]Ga-FAPI-04 mean SUV_{max} values were reported in patients with luminal A, luminal B HER2-negative, luminal B HER2-positive, HER-2-enriched, and triple-negative: 10.1 (± 5.6); 11.5 (± 5.4); 21.2 (± 8.3); 17.9 (± 6.0); 11.1 (± 4.1), respectively (p = 0.009). They specified that no difference among the luminal subtypes was found [18]. Similarly, in our cohort

Table 3 Comparison of [^{68}Ga]Ga-FAPI-46 and [^{18}F]FDG uptake per involved region according to the expression of hormone receptors (luminal-like vs. HER2-positive)

Involved regions		[^{68}Ga]Ga-FAPI-46 uptake						[^{18}F]FDG uptake					
		Luminal SUV_{max}	**HER2 SUV_{max}**	***p*-value**	**Luminal TLR_{peak}**	**HER2 TLR_{peak}**	***p*-value**	**Luminal SUV_{max}**	**HER2 SUV_{max}**	***p*-value**	**Luminal TLR_{peak}**	**HER2 TLR_{peak}**	***p*-value**
Breast		**9.6 ± 0.8**	15.8 ± 4.8	0.2	**4.1 ± 0.1**	6.6 ± 4.1	0.8	**20.8 ± 23.3**	7.7 ± 5.5	1.0	**7.5 ± 9.2**	2.5 ± 0.7	1.0
Local lymph nodes		10.5	10.1 ± 9.1	1.0	**5.1**	2.8 ± 1.8	1.0	8.9 ± 0.8	4.8 ± 1.9	1.0	**1.1 ± 1.5**	1.5 ± 1.1	0.8
M1	Distant lymph nodes	8.3 ± 8.3	6.9 ± 3.5	1.0	5.1 ± 4.3	2.6 ± 1.1	1.0	12.7	8.5 ± 6.3	1.0	4.3	1.7 ± 1.5	1.0
	Bone	15.2 ± 4.7	3.3	0.5	**9.3 ± 5.9**	1.6	0.5	10.9 ± 5.9	2.8	0.5	**2.7 ± 2.3**	0.9	1.0
	Peritoneum	7.6 ± 6.3			**7.5 ± 6.6**			6.5 ± 2.5			**1.7 ± 0.7**		
	Liver	3.1			1.6			5.3			1.7		
	Adrenal	8.6			4.9			11.4			3.5		
	Soft tissue	**7.6**			**3.2**			**42.3**			**14**		
	Lung		5.5			2.2			6.9			1.2	

Data are presented as mean ± SD (median and min-max are provided in supplementary material: supplementary Table 3). Bold highlight percentage differences between [^{68} Ga]Ga-FAPI-46 and [^{18} F]FDG uptake ≥ 50% for each involved region according to the expression of hormone receptors (supplementary material: supplementary Table 4).

we found a mean [^{68}Ga]Ga-FAPI-46 SUV_{max} of 9.6 (± 0.8) in luminal-like and 15.8 (± 4.8) in HER2-positive patients. In another retrospective study of 19 patients with invasive breast cancer (18 undergoing initial staging and one restaging after treatment for distant metastases), Furthermore, Backhaus et al. [39] found no association between [^{68}Ga]Ga-FAPI-46 uptake and tumour grade, receptor status, or histological subtype.

Moreover, the known difficulty in diagnosing cerebral and peritoneal carcinomatosis by [^{18}F]FDG, may be in favour of using FAP, mainly due to its low physiological background uptake in the brain and intestines [40–43].

Having in mind the small sample size, in which the uptake patterns may be heavily influenced by individual patients, limiting generalizability, our findings support the use of [^{68}Ga]Ga-FAPI-46 across all subgroups due to comparable uptake patterns in [^{68}Ga]Ga-FAPI-46- and [^{18}F]FDG-positive breast cancer lesions, alongside several practical advantages. These include a more patient-friendly protocol - eliminating the need for pre-imaging preparation (such as fasting for at least 4 h, and resting in a warm and quiet environment for 60 min before [^{18}F]FDG PET/CT [32]) and allowing for a shorter interval between tracer injection and image acquisition -as well as promising theranostic applications in combination with radioligand therapy [13, 25]. FAPI-46 contains a DOTA-chelator which enables binding of Ga-68, Y-90, or Lu-177 and it is one of the most common agents used for therapy purposes [44]. The theranostic field is rapidly evolving, with significant future developments anticipated, including the use of peptide-based compounds (^{68}Ga/^{177}Lu-FAP-2286) and dimeric FAPI derivatives (^{68}Ga/^{177}Lu-DOTAGA.(SA.FAPi)$_2$), which are expected to offer longer tumour retention times and, consequently, higher absorbed doses in therapeutic applications [45, 46]. Several FAP tracers with different chemical structure, binding affinity, and internalization rates, have been investigated with the aim to achieve better performance in imaging and therapy purposes [47]. Currently, [^{68}Ga]GaFAPI-04 and – 46 are the most used FAP tracers worldwide [47]. Considering that [^{68}Ga]-labelling has limitations related to its shorter half-life and restricted synthesis capacity, [^{18}F]- or [^{99m}Tc]-labelled FAPI compounds ([^{18}F]-FAPI-74 for PET, [^{99m}Tc]Tc-FAPI-34 for SPECT imaging) have also been explored [48–50]. These compounds enable wider clinical use because of the isotopes longer half-life [44]. Other promising methods to improve FAP biodistribution include albumin binding, targeting peptides or peptidomimetic compounds (such as OncoFAP, BiOncoFAP, FAP-2286 [23, 45, 51–53]) and modifying the quinoline-based structure (ex. DOTA.(SA.FAPi)2 and DOTAGA.(SA.FAPi)2 [13, 46, 54]).

In the coming years, diagnostic work-up is likely to be further complemented by subtype-specific tracers such as [^{18}F]FES or radiolabelled anti-HER2 agents, each of which may provide distinct additional diagnostic value in breast cancer [9–11, 55, 56]. Nevertheless, their availability and cost still limit its use in clinical practice. These tracers can only be used in specific histological subtypes, contrary to FAP tracers which may evaluate different tumour regions within the same patient, making it more universal for staging, even at initial diagnosis (and prior to histology).

We acknowledge that the limitations of this study are related to its small sample size that severely limits statistical power and generalizability, lack of histopathological confirmation, follow-up information and impact evaluation on clinical management, as well as a potential selection bias arising from the referral pathway.

Conclusion

In this small exploratory cohort, the head-to-head comparison of [^{68}Ga]Ga-FAPI-46 and [^{18}F]FDG PET/CT in hormone receptor and/or HER2-positive breast cancer suggests comparable uptake patterns in [^{68}Ga]Ga-FAPI-46- and [^{18}F]FDG-positive breast cancer lesions among all subtypes. These results may motivate future research of FAP theranostics in patients with breast cancer.

Abbreviations

[^{68}Ga]FAPI	Fibroblast activation protein inhibitor labelled with gallium-68
[^{18}F]FDG – 2	[^{18}F]fluoro-2-deoxy-D-glucose labelled with fluoride-18
HER2	Human epidermal growth factor receptor 2
SUV	Standardized uptake value
TLR	Tumour-liver ratio
UICC	Union for International cancer control

Supplementary Information

The online version contains supplementary material available at https://doi.org/10.1186/s13550-026-01390-3.

Supplementary Material 1

Acknowledgements

Not applicable.

Author contributions

Conceptualization – ATK, SCV, KH, WPF; SKand DK; Methodology – ATK, SCV and DK; Data collection – ATK; Data analysis – ATK, SCV, DK; Writing – ATK, SCV, DK. KMP IC, IAM, RH, AW, NH, PC, LD, RS, LU, MS, KH, WPF, and SK contributed to the study design and critically revised the manuscript. All authors approved its final content.

Funding

Open Access funding enabled and organized by Projekt DEAL. This research was partly funded by the Clinician Scientist Program of the University Medicine Essen Clinician Scientist Academy (UMEA; Faculty of Medicine and DFG), FU 356/12 – 2., Prostate Cancer Foundation TACTICAL Award No 22TACT01.

Data availability

Complementary information and analysis are provided as supplementary material. The datasets used and/or analysed during the current study are available from the corresponding author on reasonable request.

Declarations

Ethics approval and consent to participate

The ethics committee from the University of Duisburg–Essen, medical faculty approved the study (ethics protocol permits 19-8991-BO and 20-9485-BO).

Consent for publication

Not applicable.

Competing interests

Alina T. Küper was supported by the Clinician Scientist Program of the University Medicine Essen Clinician Scientist Academy (UMEA; Faculty of Medicine and DFG), FU 356/12 – 2. Anja Welt has received travel support from Pfizer and Lilly; is a member of the steering committee in the Breast cancer and Gynaecological cancer Track of the AIO (Arbeitsgemeinschaft Internistische Onkologie), of the DKG (Deutsche Krebsgesellschaft), and member of the Consensus Conference Update S3-Guideline Breast Cancer of the DKG; participated in advisory boards for MSD, Roche, Novartis, Pfizer, Seagen, Lilly, Menarini Stemline, Pierre Fabre; participated on a data safety monitoring board for iOMEDICO; received honoraria for lectures/presentations from Roche, Eisai, Novartis, Pfizer, Lilly, Iomedico, Interplan, MSD, MCI, RCC, all outside of the submitted work. Ilectra A. Mavroeidi was supported by the Clinician Scientist Program of the University Medicine Essen Clinician Scientist Academy (UMEA; Faculty of Medicine and DFG), FU 356/12 – 2. Rainer Hamacher was supported by the Clinician Scientist Program of the University Medicine Essen Clinician Scientist Academy (UMEA; Faculty of Medicine and DFG), FU 356/12 – 2.; reports travel grants from Lilly, Novartis, and PharmaMar; and reports personal fees from Lilly and PharmaMar, all outside the submitted work. Kim M. Pabst was supported by the Clinician Scientist Program of the University Medicine Essen Clinician Scientist Academy (UMEA; Faculty of Medicine and DFG), FU 356/12 – 2; reports travel fees from IPSEN; and reports research funding from Bayer, as well as travel support and consultant fees from Novartis, all outside the submitted work. Robert Seifert has received research/travel support from Boehringer Ingelheim Fund and Else Kröner-Fresenius-Stiftung, as well as travel support and lecture fees from Novartis and Boston Scientific, all outside the submitted work. Lale Umutlu is a Speaker/Advisory Board Member for Bayer Healthcare and Siemens Healthcare and received research grants from Siemens Healthcare, all outside of the submitted work. Martin Schuler reports personal fees as a consultant from Amgen, AstraZeneca, Boehringer Ingelheim, Bristol Myers Squibb, GlaxoSmithKline, Janssen, Merck Serono, Novartis, Roche, Sanofi, and Takeda; honoraria for continuing medical education presentations from Amgen, Boehringer Ingelheim, Bristol Myers Squibb, Janssen, MSD, and Novartis; and research funding (to the institution) from AstraZeneca and Bristol Myers Squibb, all outside the submitted work. Ken Herrmann reports personal fees from Bayer, personal fees and other from Sofie Biosciences, personal fees from SIRTEX, non-financial support from ABX, personal fees from Adacap, personal fees from Curium, personal fees from Endocyte, grants and personal fees from BTG, personal fees from IPSEN, personal fees from Siemens Healthineers, personal fees from GE Healthcare, personal fees from Amgen, personal fees from Novartis, personal fees from ymabs, personal fees from Aktis Oncology, personal fees from Theragnostics, personal fees from Pharma15, all outside the submitted work. Wolfgang P. Fendler reports fees from SOFIE Bioscience (research funding), Janssen (consultant, speaker), Perceptive (consultant, image review), Bayer (consultant, speaker, research funding), Novartis (speaker, consultant), Telix (speaker), GE Healthcare (speaker, consultant), Eczacıbaşı Monrol (speaker), Abx (speaker), Amgen (speaker, research funding), Urotrials (speaker), Lilly (consultant), AstraZeneca (research funding), all outside of the submitted work. Sherko Kümmel reports a consultant or advisory role with Roche/Genentech, Genomic Health, Novartis, AstraZeneca, Amgen, Celgene, SOMATEX, Daiichi Sankyo, pfm medical, Pfizer, MSD Oncology, Lilly, Sonoscape, Gilead Sciences, Seagen, and Agendia. He also reports travel support and expenses from Roche, Daiichi Sankyo, and Gilead Sciences and an uncompensated relationship with WSG, all outside the submitted work. David Kersting reports fees from GE Healthcare (consultant, travel grants), Life Molecular Imaging and Sanofi (travel grants), Novartis (speaker), Pfizer (speaker, research funding), and funding by the German Research Foundation (DFG, KE2933/1–1), all outside the submitted work.

Author details

[1]Department of Nuclear Medicine and German Cancer Consortium (DKTK), University Hospital Essen, University of Duisburg-Essen, Essen, Germany
[2]Department of Nuclear Medicine and Radiopharmacology, Champalimaud Clinical Center, Champalimaud Foundation, Lisbon, Portugal
[3]Department of Radiology, Leiden University Medical Center, Leiden, The Netherlands
[4]Department of Medical Oncology, NCT site, University Hospital Essen, West German Cancer Center, University of Duisburg-Essen, Essen, Germany
[5]German Cancer Consortium (DKTK), Partner Site University Hospital Essen, Essen, Germany
[6]Nuclear Medicine Department, LRB, CHU Grenoble Alpes, INSERM, Université Grenoble Alpes, Grenoble, France
[7]Department of Nuclear Medicine, University Hospital Bern, University of Bern, Bern, Switzerland
[8]Institute of Interventional and Diagnostic Radiology and Neuroradiology, University Hospital Essen, University of Duisburg-Essen, Essen, Germany
[9]Breast Unit Essen, Kliniken Essen-Mitte, Essen, Germany

Received: 9 September 2025 / Accepted: 10 February 2026
Published online: 13 March 2026

References

1. Bray F, Laversanne M, Sung H, Ferlay J, Siegel RL, Soerjomataram I, et al. Global cancer statistics 2022: GLOBOCAN estimates of incidence and mortality worldwide for 36 cancers in 185 countries. CA Cancer J Clin. 2024;74(3):229–63.
2. Kim J, Harper A, McCormack V, Sung H, Houssami N, Morgan E, et al. Global patterns and trends in breast cancer incidence and mortality across 185 countries. Nat Med. 2025. https://doi.org/10.1038/s41591-025-03502-3.
3. Yersal O, Barutca S. Biological subtypes of breast cancer: prognostic and therapeutic implications. World J Clin Oncol. 2014;5(3):412–24.
4. Orrantia-Borunda E, Anchondo-Nuñez P, Acuña-Aguilar LE, Gómez-Valles FO, Ramírez-Valdespino CA. Subtypes of Breast Cancer. In: Mayrovitz HN, editor. Breast Cancer. Brisbane (AU): Exon Publications Copyright: The Authors.; The authors confirm that the materials included in this chapter do not violate copyright laws. Where relevant, appropriate permissions have been obtained from the original copyright holder(s), and all original sources have been appropriately acknowledged or referenced.; 2022.
5. Giuliano AE, Connolly JL, Edge SB, Mittendorf EA, Rugo HS, Solin LJ, et al. Breast cancer-Major changes in the American joint committee on cancer eighth edition cancer staging manual. CA Cancer J Clin. 2017;67(4):290–303.
6. Vaz SC, Woll JPP, Cardoso F, Groheux D, Cook GJR, Ulaner GA, et al. Joint EANM-SNMMI guideline on the role of 2-[(18)F]FDG PET/CT in no special type breast cancer: (endorsed by the ACR, ESSO, ESTRO, EUSOBI/ESR, and EUSOMA). Eur J Nucl Med Mol Imaging. 2024;51(9):2706–32.
7. Avril N, Rosé CA, Schelling M, Dose J, Kuhn W, Bense S, et al. Breast imaging with positron emission tomography and fluorine-18 fluorodeoxyglucose: use and limitations. J Clin Oncol. 2000;18(20):3495–502.
8. Groheux D, Giacchetti S, Moretti JL, Porcher R, Espié M, Lehmann-Che J, et al. Correlation of high 18F-FDG uptake to clinical, pathological and biological prognostic factors in breast cancer. Eur J Nucl Med Mol Imaging. 2011;38(3):426–35.
9. Mankoff D, Balogová S, Dunnwald L, Dehdashti F, DeVries E, Evangelista L, et al. Summary: SNMMI procedure Standard/EANM practice guideline for Estrogen receptor imaging of patients with breast cancer using 16α-[(18)F] Fluoro-17β-Estradiol PET. J Nucl Med. 2024;65(2):221–3.
10. Eisses B, van Geel JJL, Brouwers AH, Bensch F, Elias SG, Kuip EJM, et al. Whole-body HER2 heterogeneity identified on HER2 PET in HER2-negative, -low, and -positive metastatic breast cancer. J Nucl Med. 2024;65(10):1540–7.
11. Mileva M, de Vries EGE, Guiot T, Wimana Z, Deleu AL, Schröder CP, et al. Molecular imaging predicts lack of T-DM1 response in advanced HER2-positive breast cancer (final results of ZEPHIR trial). NPJ Breast Cancer. 2024;10(1):4.

12. Parihar AS, Vaz S, Sutcliffe S, Pant N, Schoones JW, Ulaner GA. (18)F-Fluoroestradiol PET/CT for Predicting Benefit from Endocrine Therapy in Patients with Estrogen Receptor-Positive breast cancer: A Systematic Review and Meta nalysis. J Nucl Med. 2025;66(5):692-9.https://doi.org/10.2967/jnumed.124.269163.
13. Mori Y, Novruzov E, Schmitt D, Cardinale J, Watabe T, Choyke PL, et al. Clinical applications of fibroblast activation protein inhibitor positron emission tomography (FAPI-PET). NPJ Imaging. 2024;2(1):48.
14. Evangelista L, Filippi L, Schillaci O. What radiolabeled FAPI pet can add in breast cancer? A systematic review from literature. Ann Nucl Med. 2023;37(8):442–50.
15. Gilardi L, Airò Farulla LS, Demirci E, Clerici I, Omodeo Salè E, Ceci F. Imaging cancer-associated fibroblasts (CAFs) with FAPi PET. Biomedicines. 2022. https://doi.org/10.3390/biomedicines10030523.
16. Taralli S, Lorusso M, Perrone E, Perotti G, Zagaria L, Calcagni ML. PET/CT with fibroblast activation protein inhibitors in breast cancer: diagnostic and theranostic application-a literature review. Cancers (Basel). 2023. https://doi.org/10.3390/cancers15030908.
17. Kömek H, Can C, Güzel Y, Oruç Z, Gündoğan C, Yildirim ÖA. 68Ga-FAPI-04 PET/CT, a new step in breast cancer imaging: a comparative pilot study with the 18F-FDG PET/CT. Ann Nucl Med. 2021;35(6):744–52.
18. Elboga U, Sahin E, Kus T, Cayirli YB, Aktas G, Uzun E, et al. Superiority of (68)Ga-FAPI PET/CT scan in detecting additional lesions compared to (18)FDG PET/CT scan in breast cancer. Ann Nucl Med. 2021;35(12):1321–31.
19. Dendl K, Koerber SA, Finck R, Mokoala KMG, Staudinger F, Schillings L. 68Ga-FAPI-PET/CT in patients with various gynecological malignancies. Eur J Nucl Med Mol Imaging. 2021;48(12):4089–100.
20. Ballal S, Yadav MP, Moon ES, Kramer VS, Roesch F, Kumari S, et al. Biodistribution, pharmacokinetics, dosimetry of [(68)Ga]Ga-DOTA.SA.FAPi, and the head-to-head comparison with [(18)F]F-FDG PET/CT in patients with various cancers. Eur J Nucl Med Mol Imaging. 2021;48(6):1915–31.
21. Zheng S, Lin J, Zhu Y, Chen Y, Zhang J, Chen X, et al. 68Ga-FAPI versus 18F-FDG PET/CT in evaluating newly diagnosed breast cancer patients: A Head-to-Head comparative study. Clin Nucl Med. 2023;48(3):e104–9.
22. Yadav MP, Ballal S, Martin M, Roesch F, Satapathy S, Moon ES, et al. Therapeutic potential of [(177)Lu]Lu-DOTAGA-FAPi dimers in metastatic breast cancer patients with limited treatment options: efficacy and safety assessment. Eur J Nucl Med Mol Imaging. 2024;51(3):805–19.
23. Baum RP, Schuchardt C, Singh A, Chantadisai M, Robiller FC, Zhang J, et al. Feasibility, Biodistribution, and preliminary dosimetry in Peptide-Targeted radionuclide therapy of diverse adenocarcinomas using (177)Lu-FAP-2286: First-in-Humans results. J Nucl Med. 2022;63(3):415–23.
24. Assadi M, Rekabpour SJ, Jafari E, Divband G, Nikkholgh B, Amini H, et al. Feasibility and therapeutic potential of 177Lu-Fibroblast activation protein Inhibitor-46 for patients with relapsed or refractory cancers: A preliminary study. Clin Nucl Med. 2021;46(11):e523–30.
25. Privé BM, Boussihmad MA, Timmermans B, van Gemert WA, Peters SMB, Derks YHW, et al. Fibroblast activation protein-targeted radionuclide therapy: background, opportunities, and challenges of first (pre)clinical studies. Eur J Nucl Med Mol Imaging. 2023;50(7):1906–18.
26. Sahin E, Kus T, Aytekin A, Uzun E, Elboga U, Yilmaz L, et al. (68)Ga-FAPI PET/CT as an alternative to (18)F-FDG PET/CT in the imaging of invasive lobular breast carcinoma. J Nucl Med. 2024;65(4):512–9.
27. Eshet Y, Tau N, Apter S, Nissan N, Levanon K, Bernstein-Molho R, et al. The role of 68 Ga-FAPI PET/CT in detection of metastatic lobular breast cancer. Clin Nucl Med. 2023;48(3):228–32.
28. Abe K, Watabe T, Kaneda-Nakashima K, Shirakami Y, Kadonaga Y, Naka S, et al. Evaluation of targeted alpha therapy using [(211)At]FAPI1 in triple-negative breast cancer xenograft models. Int J Mol Sci. 2024. https://doi.org/10.3390/ijms252111567.
29. Liu T, Liu J, Liu J, Xu S, Yu J. [18F]AlF-NOTA-FAPI-04 PET/CT Uptake of the Primary Tumor on PET/CT Imaging Might Distinguish Triple Negative Breast Cancer.
30. Weber M, Jentzen W, Hofferber R, Herrmann K, Fendler WP, Conti M, et al. Evaluation of [(68)Ga]Ga-PSMA PET/CT images acquired with a reduced scan time duration in prostate cancer patients using the digital biograph vision. EJNMMI Res. 2021;11(1):21.
31. O JH, Lodge MA, Wahl RL. Practical PERCIST: a simplified guide to PET response criteria in solid tumors 1.0. Radiology. 2016;280(2):576–84.
32. Boellaard R, Delgado-Bolton R, Oyen WJ, Giammarile F, Tatsch K, Eschner W, et al. FDG PET/CT: EANM procedure guidelines for tumour imaging: version 2.0. Eur J Nucl Med Mol Imaging. 2015;42(2):328–54.
33. Kitajima K, Fukushima K, Miyoshi Y, Nishimukai A, Hirota S, Igarashi Y, et al. Association between ^{18}F-FDG uptake and molecular subtype of breast cancer. Eur J Nucl Med Mol Imaging. 2015;42(9):1371–7.
34. Antunovic L, Gallivanone F, Sollini M, Sagona A, Invento A, Manfrinato G, et al. [(18)F]FDG PET/CT features for the molecular characterization of primary breast tumors. Eur J Nucl Med Mol Imaging. 2017;44(12):1945–54.
35. Guo W, Xu W, Meng T, Fan C, Fu H, Pang Y, et al. FAP-targeted PET/CT imaging in patients with breast cancer from a prospective bi-center study: insights into diagnosis and clinic management. Eur J Nucl Med Mol Imaging. 2025;52(7):2317–34.
36. Salimifard S, Masjedi A, Hojjat-Farsangi M, Ghalamfarsa G, Irandoust M, Azizi G, et al. Cancer associated fibroblasts as novel promising therapeutic targets in breast cancer. Pathol Res Pract. 2020;216(5):152915.
37. de Mooij CM, Ploumen RAW, Nelemans PJ, Mottaghy FM, Smidt ML, van Nijnatten TJA. The influence of receptor expression and clinical subtypes on baseline [18F]FDG uptake in breast cancer: systematic review and meta-analysis. EJNMMI Res. 2023;13(1):5.
38. Liu T, Xu S, Cheng K, Pei J, Wang S, Li C, et al. Exploring the value of FAP-targeted PET/CT in differentiating breast cancer molecular subtypes: a preliminary study. Eur J Nucl Med Mol Imaging. 2024;52(1):280–90.
39. Backhaus P, Burg MC, Roll W, Büther F, Breyholz H-J, Weigel S, et al. Simultaneous FAPI PET/MRI targeting the Fibroblast-Activation protein for breast cancer. Radiology. 2021;302(1):39–47.
40. Santos L, Moreira JN, Abrunhosa A, Gomes C. Brain metastasis: an insight into novel molecular targets for theranostic approaches. Crit Rev Oncol Hematol. 2024;198:104377.
41. Liu Y, Ding H, Cao J, Liu G, Chen Y, Huang Z. [(68)Ga]Ga-FAPI PET/CT in brain tumors: comparison with [(18)F]F-FDG PET/CT. Front Oncol. 2024;14:1436009.
42. Fu C, Zhang B, Guo T, Li J. Imaging evaluation of peritoneal metastasis: current and promising techniques. Korean J Radiol. 2024;25(1):86–102.
43. Zhang Y, Xu M, Wang Y, Yu F, Chen X, Wang G, et al. Characteristics of (18)F-FAPI-04 PET/CT in patients with peritoneal metastasis and to predict treatment efficacy, a head-to-head comparison with (18)F-FDG PET/CT. Cancer Imaging. 2025;25(1):66.
44. Mori Y, Kratochwil C, Haberkorn U, Giesel FL. Fibroblast activation protein inhibitor theranostics: early clinical translation. PET Clin. 2023;18(3):419–28.
45. Zboralski D, Hoehne A, Bredenbeck A, Schumann A, Nguyen M, Schneider E, et al. Preclinical evaluation of FAP-2286 for fibroblast activation protein targeted radionuclide imaging and therapy. Eur J Nucl Med Mol Imaging. 2022;49(11):3651–67.
46. Ballal S, Yadav MP, Moon ES, Kramer VS, Roesch F, Kumari S, et al. First-in-human results on the biodistribution, pharmacokinetics, and dosimetry of [(177)Lu]Lu-DOTA.SA.FAPi and [(177)Lu]Lu-DOTAGA.(SA.FAPi)(2). Pharmaceuticals (Basel). 2021. https://doi.org/10.3390/ph14121212.
47. Mori Y, Dendl K, Cardinale J, Kratochwil C, Giesel FL, Haberkorn U. FAPI PET: fibroblast activation protein inhibitor use in oncologic and nononcologic disease. Radiology. 2023;306(2):e220749.
48. Giesel FL, Adeberg S, Syed M, Lindner T, Jiménez-Franco LD, Mavriopoulou E, et al. FAPI-74 PET/CT using either (18)F-AlF or Cold-Kit (68)Ga labeling: Biodistribution, radiation Dosimetry, and tumor delineation in lung cancer patients. J Nucl Med. 2021;62(2):201–7.
49. Lindner T, Altmann A, Giesel F, Kratochwil C, Kleist C, Krämer S, et al. (18)F-labeled tracers targeting fibroblast activation protein. EJNMMI Radiopharm Chem. 2021;6(1):26.
50. Lindner T, Altmann A, Krämer S, Kleist C, Loktev A, Kratochwil C, et al. Design and development of (99m)Tc-labeled FAPI tracers for SPECT imaging and (188)Re therapy. J Nucl Med. 2020;61(10):1507–13.
51. Millul J, Bassi G, Mock J, Elsayed A, Pellegrino C, Zana A, et al. An ultra-high-affinity small organic ligand of fibroblast activation protein for tumor-targeting applications. Proc Natl Acad Sci U S A. 2021. https://doi.org/10.1073/pnas.2101852118.
52. Backhaus P, Gierse F, Burg MC, Büther F, Asmus I, Dorten P, et al. Translational imaging of the fibroblast activation protein (FAP) using the new ligand [(68)Ga]Ga-OncoFAP-DOTAGA. Eur J Nucl Med Mol Imaging. 2022;49(6):1822–32.
53. Millul J, Koepke L, Haridas GR, Sparrer KMJ, Mansi R, Fani M. Head-to-head comparison of different classes of FAP radioligands designed to increase

tumor residence time: monomer, dimer, albumin binders, and small molecules vs peptides. Eur J Nucl Med Mol Imaging. 2023;50(10):3050–61.
54. Moon ES, Elvas F, Vliegen G, De Lombaerde S, Vangestel C, De Bruycker S, et al. Targeting fibroblast activation protein (FAP): next generation PET radiotracers using squaramide coupled bifunctional DOTA and DATA(5m) chelators. EJNMMI Radiopharm Chem. 2020;5(1):19.
55. Ulaner GA, Jhaveri K, Chandarlapaty S, Hatzoglou V, Riedl CC, Lewis JS, et al. Head-to-Head evaluation of (18)F-FES and (18)F-FDG PET/CT in metastatic invasive lobular breast cancer. J Nucl Med. 2021;62(3):326–31.
56. Gebhart G, Lamberts LE, Wimana Z, Garcia C, Emonts P, Ameye L, et al. Molecular imaging as a tool to investigate heterogeneity of advanced HER2-positive breast cancer and to predict patient outcome under trastuzumab emtansine (T-DM1): the ZEPHIR trial. Ann Oncol. 2016;27(4):619–24.

Publisher's note